

Elastic systems with correlated disorder: Response to tilt and application to surface growth

Andrei A. Fedorenko

CNRS-Laboratoire de Physique Théorique de l'École Normale Supérieure, 24 rue Lhomond, 75231 Paris, France

(Dated: December 5, 2007)

We study elastic systems such as interfaces or lattices pinned by correlated quenched disorder considering two different types of correlations: generalized columnar disorder and quenched defects correlated as $\sim x^{-a}$ for large separation x . Using functional renormalization group methods, we obtain the critical exponents to two-loop order and calculate the response to a transverse field h . The correlated disorder violates the statistical tilt symmetry resulting in nonlinear response to a tilt. Elastic systems with columnar disorder exhibit a transverse Meissner effect: disorder generates the critical field h_c below which there is no response to a tilt and above which the tilt angle behaves as $\vartheta \sim (h - h_c)^\phi$ with a universal exponent $\phi < 1$. This describes the destruction of a weak Bose glass in type-II superconductors with columnar disorder caused by tilt of the magnetic field. For isotropic long-range correlated disorder, the linear tilt modulus vanishes at small fields leading to a power-law response $\vartheta \sim h^\phi$ with $\phi > 1$. The obtained results are applied to the Kardar-Parisi-Zhang equation with temporally correlated noise.

PACS numbers: 74.25.Qt, 75.60.Ch, 81.10.-h

I. INTRODUCTION

Elastic objects in disordered media are a fruitful concept to study diverse physical systems such as domain walls in ferromagnets,¹ charge density waves in solids (CDW),² and vortices in type-II superconductors.³ In all these systems, the interplay between elasticity, which tends to keep the object ordered (flat or periodic), and disorder, which induces distortions, produces a complicated energy landscape.^{4,5,6} This leads to rich glassy behavior. For instance, at low temperature, weak defects in a crystal of type-II superconductor, such as oxygen vacancies, can collectively pin the flux lines in the so-called Bragg glass state.⁷ Vortex pinning prevents the dissipation of energy, and thus, its understanding has a great importance for applications. It was observed in experiments that columnar defects produced in the underlying lattice of superconductors by heavy ion irradiation can significantly enhance vortex pinning.⁸ Nelson and Vinokur⁹ mapped the problem of flux lines pinned by columnar defects onto the quantum problem of bosons with uncorrelated quenched disorder in one dimension less. The mapping predicts a low temperature “strong” Bose-glass phase which corresponds to the localization of bosons in a random potential provided the longitudinal applied field H_{\parallel} is weak enough to create vortices with density smaller than the density of pins. For larger H_{\parallel} , the Bose-glass can coexist with a resistive liquid of interstitial vortices which, it is argued, can freeze upon cooling into a collectively pinned weak Bose-glass phase.¹⁰ At low tilts of the applied magnetic field relative to the parallel columnar defects, flux lines remain localized along the defects, so that vortices are characterized by an infinite tilt modulus. This phenomenon which is known as the transverse Meissner effect has been extensively studied experimentally.¹¹ Vortices undergo a delocalization transition to a flux liquid state at some finite critical mismatch angle ϑ_c between the applied field and the

direction of defect alignment, i.e., at some finite transverse field H_{\perp}^c . The schematic phase diagram is shown in Fig. 1. The breakdown of the transverse Meissner effect above H_{\perp}^c can be described by

$$B_{\perp} \sim (H_{\perp} - H_{\perp}^c)^\phi, \quad (1)$$

where B_{\perp} is the transverse magnetic induction due to the tilted flux lines. Heuristic arguments of Ref. 12 based on kink statistics predict $\phi = 1/2$ in $d = 1 + 1$ dimensions and $\phi = 3/2$ in $d = 2 + 1$. However, experiments on a bulk superconductor ($d = 3$) with columnar disorder find $\phi \approx 0.5$,¹³ while the strong-randomness real-space renormalization group suggests $\phi = 1$ in $d = 2$,¹⁴ that is in disagreement with the predictions based on kink statistics. Thus, further investigations are needed.

The theoretical advances for elastic objects in disordered media are achieved by developing two general methods: the Gaussian variational approximation (GVA) and the functional renormalization group (FRG). GVA relies on the replica method allowing for the replica symmetry breaking.¹⁵ It is exact in the mean field limit, i.e., in the limit of a large number of components. FRG is a perturbative renormalization group method which is able to handle infinite number of relevant operator.¹⁶ Simple scaling arguments show that the large-scale properties of a d -dimensional elastic system are governed by uncorrelated disorder in $d < d_{uc} = 4$. In particular, displacements grow unboundedly with distance, resulting in a roughness of interfaces or distortions of periodic structures. The problem is notably difficult due to the so-called dimensional reduction which states that a d -dimensional disordered system at zero temperature is equivalent to all orders in perturbation theory to a pure system in $d - 2$ dimensions at finite temperature. However, metastability renders the zero-temperature perturbation theory useless: it breaks down on scales larger than the so-called Larkin length.¹⁷ The peculiarity of the problem is that for $d < d_{uc}$ there is an infinite

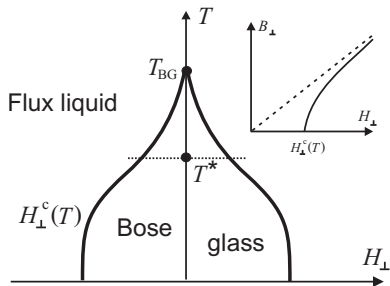


FIG. 1: Phase diagram of flux lines with columnar disorder at a fixed applied field H_{\parallel} parallel to the columns as a function of transverse field H_{\perp} and temperature T . The Bose glass corresponds to vortex localization and exhibits a transverse Meissner effect. The transition to liquid phase occurs at the critical field $H_{\perp}^c(T)$. In (1+1) dimensions, the temperatures T_{BG} and T^* are related to the special values of the Luttinger interaction parameter: $g(T_{\text{BG}}) = 3/2$ and $g(T^*) = 1$. The inset shows the response to a transverse field in the vicinity of transition.

set of relevant operators. They can be parametrized by a function which is nothing but the disorder correlator. The renormalized disorder correlator becomes a nonanalytic function beyond the Larkin scale.¹⁶ The appearance of a nonanalyticity in the form of a cusp at the origin is related to metastability, and nicely accounts for the generation of a threshold force at the depinning transition.^{18,19,20,21} It was recently shown that FRG can unambiguously be extended to higher loop order so that the underlining nonanalytic field theory is probably renormalizable to all orders.^{22,23,24} Although the two methods, GVA and FRG, are very different, they provide a fairly consistent picture and recently a relation between them was established.²⁵ There is also good agreement with results of numerical simulations, not only for critical exponents^{26,27,28} but also for distributions of observables^{29,30} and the effective action.³¹

The FRG techniques were also applied to pinning of elastic systems by columnar disorder.^{32,33,34} The models studied by FRG, though that may be more directly applicable to systems such as charge density waves or domain walls, exhibit many features of the Bose-glass phase of type-II superconductors. In particular, they demonstrate the absence of a response to a weak transverse field and provide a way to compute the exponent ϕ .³⁴ However, since FRG intrinsically assumes collective pinning, it also predicts a slow algebraic decay of translational order, that is not expected in the strong Bose-glass state when each vortex is pinned by a single columnar pin. Thus, the FRG is able to handle only a weak Bose-glass phase, exhibiting both the transverse Meissner effects and the Bragg peaks.

In the present paper, we extend the FRG studies to two-loop order. We also extend to two-loop order our recent work³⁵ on the elastic objects in the presence of long-range (LR) correlated disorder with correlations decaying with distance as a power law. This type of disorder can

be induced, for example, by the presence of extended defects with random orientations. In particular, we address the question of the response to a tilting field and compare the effects produced by different types of disorder correlations. The outline of this paper is as follows. Section II introduces the models of elastic objects in the presence of generalized columnar and LR-correlated disorder. In Sec. III, we study the model with LR correlated disorder using FRG up to two-loop order. In Sec. IV, we consider the response of elastic objects to a tilting field and discuss the relation to the quantum problem of interacting disordered bosons. In Sec. V, we revise the problem of surface growth with temporally correlated noise using the results obtained in the previous sections.

II. MODELS WITH CORRELATED DISORDER

The configuration of elastic object embedded in a D -dimensional space can be parametrized by an N -component displacement field u_x , where x belongs to the d -dimensional internal space. For instance, a d -dimensional domain wall corresponds to $d = D - 1$ and $N = 1$, vortices in a bulk superconductor to $d = D = 3$ and $N = 2$, and vortices confined in a slab to $d = D = 2$ and $N = 1$. In this paper, we restrict our study to the case $N = 1$ and elastic objects with short-range elasticity. In the presence of disorder, the equilibrium behavior of the elastic object is defined by the Hamiltonian

$$\mathcal{H}[u] = \int d^d x \left[\frac{c}{2} (\nabla u_x)^2 + V(x, u_x) \right], \quad (2)$$

where c is the elasticity and $V(x, u)$ is a random Gaussian potential, with zero mean and variance that will be defined below. We denote everywhere below $\int_q = \int \frac{d^d q}{(2\pi)^d}$ and $\int_x = \int d^d x$. The short-scale UV cutoff is implied at $q \sim \Lambda$ and the system size is L . The random potential causes the interface to wander and become rough with displacements growing with the distance x as $C(x) \sim x^{2\zeta}$. Here, ζ is the roughness exponent. Elastic periodic structures lose their strict translational order and exhibit a slow logarithmic growth of displacements, $C(x) = \mathcal{A}_d \ln |x|$. Although most results of the paper concern the statics at equilibrium, it is instructive to give a dynamic formulation of the problem. The driven dynamics of the elastic object in a disordered medium at zero temperature can be described by the following overdamped equation of motion

$$\eta \partial_t u_{xt} = c \nabla^2 u_{xt} + F(x, u_{xt}) + f. \quad (3)$$

Here, η is the friction coefficient, $F = -\partial_u V(x, u)$ the pinning force, and f the applied force. The system undergoes the so-called depinning transition at the critical force f_c , which separates sliding and pinned states. Upon approaching the depinning transition from the sliding state $f \rightarrow f_c^+$ the center-of-mass velocity $v =$

$L^{-d} \int_x \partial_t u_{xt}$ vanishes as a power law

$$v \sim (f - f_c)^\beta. \quad (4)$$

In the present work, we consider model (2) with two different types of correlated disorder, which are described in two subsequent sections.

A. Generalized columnar disorder

Real systems often contain extended defects in the form of linear dislocations, planar grain boundaries, three-dimensional cavities, etc. We consider the model with extended defects which can be viewed as a generalization of columnar disorder. The defects are ε_d -dimensional objects (hyperplanes) extending throughout the whole system along the coordinate x_{\parallel} and randomly distributed in the transverse directions x_{\perp} with the concentration taken to be well below the percolation limit.^{36,37,38} The corresponding correlator of the disorder potential can be written as

$$\overline{V(x, u)V(x', u')} = R(u - u')\delta^{d-\varepsilon_d}(x_{\perp} - x'_{\perp}). \quad (5)$$

The case of uncorrelated pointlike disorder corresponds to $\varepsilon_d = 0$ and the columnar disorder to $\varepsilon_d = 1$. For interfaces, one has to distinguish two universality classes: random bond (RB) disorder described by a short-range function $R(u)$ and random field (RF) disorder corresponding to a function which behaves as $R(u) \sim |u|$ at large u . Random periodic (RP) universality class corresponding to a periodic function $R(u)$ describes systems such as CDW or vortices in $d = 1 + 1$ dimensions.⁶

The standard way to average over disorder is the replica trick. Introducing n replicas of the original system we derive the replicated Hamiltonian as follows:

$$\begin{aligned} \frac{\mathcal{H}_n[u]}{T} &= \frac{1}{2T} \sum_a \int_x \left[c_{\parallel} (\nabla_{\parallel} u_x^a)^2 + c_{\perp} (\nabla_{\perp} u_x^a)^2 \right. \\ &\quad \left. + m^2 (u_x^a)^2 \right] - \frac{1}{2T^2} \sum_{a,b} \int d^{\varepsilon_d} x_{\parallel} d^{\varepsilon_d} x'_{\parallel} \\ &\quad \times d^{d-\varepsilon_d} x_{\perp} R \left(u_{x_{\parallel}, x_{\perp}}^a - u_{x'_{\parallel}, x_{\perp}}^b \right), \quad (6) \end{aligned}$$

where we have added a small mass m providing an infrared cutoff. Replica indices a and b run from 1 to n and the properties of the original disordered system can be restored in the limit $n \rightarrow 0$. We explicitly show in Hamiltonian (6) that one has to distinguish the longitudinal and transverse elasticity modules. Even if the bare elasticity tensor is isotropic, the effective elasticity may not due to the renormalization by anisotropically distributed disorder.

B. Long-range correlated disorder

In the case of isotropically distributed disorder, the power-law correlation is the simplest assumption with

possibility for scaling behavior with new fixed points (FPs) and new critical exponents. The bulk critical behavior of systems with RB and RF disorder which correlations decay as a power-law x^{-a} was studied in Refs. 39,40,41,42. The power-law correlation of disorder in the d -dimensional space with exponent $a = d - \varepsilon_d$ can be ascribed to ε_d dimensional extended defects randomly distributed with random orientation. For instance, $a = d$ corresponds to uncorrelated pointlike defects, and $a = d - 1$ ($a = d - 2$) describes infinite lines (planes) of defects with random orientation. The power-law correlation with a noninteger value $a = d - d_f$ can be found in the systems containing fractal-like structures with the fractal dimension d_f .⁴³ Here we consider the model with LR-correlated disorder introduced in Ref. 35 which is defined by the following disorder correlator:

$$\begin{aligned} \overline{V(x, u)V(x', u')} &= R_1(u - u')\delta^d(x - x') \\ &\quad + R_2(u - u')g(x - x'), \quad (7) \end{aligned}$$

with $g(x) \sim x^{-a}$. We fix the constant in the Fourier space taking $g(q) = q^{a-d}$. The first term in Eq. (7) corresponds to pointlike disorder with short-range (SR) correlations and the second term to LR-correlated disorder. *A priori* we are interested in the case $a < d$ when the correlations decay sufficiently slowly, otherwise the disorder is simply SR correlated.

Using the replica trick, we obtain the replicated Hamiltonian $\mathcal{H}_n[u]$ and the corresponding action $S[u]$:

$$\begin{aligned} S[u] &= \frac{\mathcal{H}_n[u]}{T} = \frac{1}{2T} \sum_a \int_x \left[c (\nabla u_x^a)^2 + m^2 (u_x^a)^2 \right] \\ &\quad - \frac{1}{2T^2} \sum_{a,b} \int_x R_1(u_x^a - u_x^b) \\ &\quad - \frac{1}{2T^2} \sum_{a,b} \int_{xx'} R_2(u_x^a - u_{x'}^b)g(x - x'). \quad (8) \end{aligned}$$

One could start with model (8), setting $R_1(u) = 0$. However, as was shown in Ref. 35, a nonzero $R_1(u)$ is generated under coarse graining along the FRG flow. Note that the functions $R_i(u)$ can themselves be SR, LR, or RP. The generalization of these universality classes to LR-correlated disorder is discussed in Ref. 35.

In the case of uncorrelated disorder, the system (2) exhibits the so-called statistical tilt symmetry (STS), i.e., invariance under transformation $u_x \rightarrow u_x + f_x$ with an arbitrary function f_x . The STS issues that the one-replica part of the replicated action, i.e., the elasticity, does not get corrected by disorder to all orders. The presence of LR-correlated disorder or extended defects destroys the STS, and thus allows for the renormalization of elasticity.

For a non-Gaussian distribution of disorder, higher order ($p > 2$) cumulants would generate additional terms in the action with factors of $1/T^p$ and free sums over p replicas. These terms are irrelevant in the RG sense that can be seen by power counting, and thus will be neglected from the beginning.

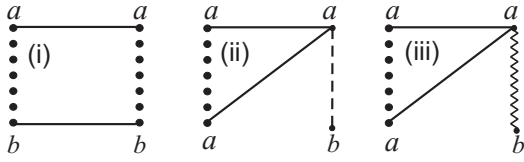


FIG. 2: Two-replica one-loop diagrams correcting disorder. The dot line corresponds to either SR disorder vertex (dashed line) or to LR disorder vertex (wavy line). Diagrams of types (i) and (ii) contribute to SR disorder. Only diagrams of type (iii) give corrections to LR disorder.

III. RENORMALIZATION OF THE MODEL WITH LONG-RANGE CORRELATED DISORDER

A. Perturbation theory and diagrammatics

We now study the scaling behavior of model (8) starting with simple power counting. The elastic term in action (8) is invariant under $x \rightarrow xb$, $u \rightarrow ub^\zeta$, $c \rightarrow b^{-\psi}c$ provided $T \rightarrow b^{\theta_T}T$ with $\theta_T = d - 2 + 2\zeta - \psi$. Since θ_T is positive near $d = 4$ the temperature T is formally irrelevant. The STS would fix $\psi = 0$, however, this is not the case here. ζ and ψ are for now undetermined and their actual values will be fixed by the disorder correlators at the stable FP. Under the rescaling transformation the disorder correlation functions R_1 and R_2 go up by factors $b^{d-2\theta_T} = b^{4-d-4\zeta+2\psi}$ and $b^{d-2\theta_T} = b^{4-a-4\zeta+2\psi}$, respectively. Thus, in the vicinity of Gaussian FP ($R_i = 0$), SR disorder becomes relevant for $\zeta - \psi/2 < (4-d)/4$ and LR disorder is naively relevant for $\zeta - \psi/2 < (4-a)/4$. *A posteriori* these inequalities are satisfied at the RB and RP FPs. For RF disorder, however, power counting suggests that SR disorder is relevant for $\zeta - \psi < (4-d)/2$, while LR disorder is relevant for $\zeta - \psi < (4-a)/2$.³⁵

Let us consider the perturbation theory in disorder and its diagrammatic representation. In momentum space, the quadratic part of action (8) gives rise to the free propagator $\langle u_a^a u_{q'}^b \rangle_0 = (2\pi)^d \delta^d(q+q') T \delta_{ab} C(q)$ represented graphically by a line:

$$a \text{ --- } b = TC(q) \delta_{ab} = \frac{T}{cq^2 + m^2} \delta_{ab}. \quad (9)$$

We will distinguish two different interactions, SR and LR, for which we adopt the following splitted diagrammatic representation:

$$\begin{array}{c} a \\ \vdots \\ b \end{array} = \sum_{ab} \frac{R_1(u_x^a - u_x^b)}{2T^2}, \quad (10)$$

$$\begin{array}{c} a \\ \text{wavy} \\ b \end{array} = \sum_{ab} \frac{R_2(u_x^a - u_{x'}^b)}{2T^2} g(x - x'). \quad (11)$$

Following the standard field theory renormalization program, we compute the effective action and determine counter-terms to render the theory UV finite as $d, a \rightarrow 4$. To regularize integrals, we use a generalized dimensional

regularization with a double expansion in $\varepsilon = 4 - d$ and $\delta = 4 - a$. The effective action $\Gamma[u]$ is defined by the Legendre transform $\Gamma[u] = Ju - W[J]$, $W'[J] = u$ of the generating functional for connected correlators $W[J] = \ln \mathcal{Z}[J]$. The replicated partition function \mathcal{Z} in the presence of sources J is given by

$$\mathcal{Z}[J] = \int \prod_a \mathcal{D}u_a \exp \left(-\mathcal{S}[u] + \int_x \sum_a J_x^a u_x^a \right). \quad (12)$$

The effective action $\Gamma[u]$ is by definition a generating functional of one-particle irreducible vertex functions. However, it turns out to be nonanalytic in some directions, and therefore, the relying on the expansion in u is danger. To overcome these difficulties, we employ the formalism of functional diagrams introduced in Ref. 24. Since the temperature is formally irrelevant, we compute the correction to the effective action at $T = 0$. Analyzing UV divergences of the functional diagrams contributing to the effective action, we find that the disorder is corrected only by local parts of two-replica diagrams and the elasticity only by one-replica diagrams.

B. Correction to disorder and β functions

To one-loop order at $T = 0$, the correction to disorder is given by the local parts of the two-replica diagrams shown in Fig. 2. The corresponding expressions read

$$\begin{aligned} \delta^1 R_1(u) &= \left[\frac{1}{2} R''_{10}(u)^2 - R''_{10}(u) R''_{10}(0) \right] I_1 \\ &\quad + [R''_{10}(u) R''_{20}(u) - R''_{10}(u) R''_{20}(0)] I_2 \\ &\quad + \frac{1}{2} R''_{20}(u)^2 I_3, \end{aligned} \quad (13)$$

$$\delta^1 R_2(u) = -R''_{20}(u) R''_{10}(0) I_1 - R''_{20}(u) R''_{20}(0) I_2, \quad (14)$$

where we have included factor of $1/c_0^2$ in $R_{i0}(u)$. In this section, bare parameters are denoted by the subscript “0”. The one-loop integrals I_1 , I_2 and I_3 diverge logarithmically and for $\varepsilon, \delta \rightarrow 0$ are given by

$$I_1 = \int_q \frac{1}{(q^2 + \hat{m}^2)^2} = K_4 \frac{\hat{m}^{-\varepsilon}}{\varepsilon} + \mathcal{O}(1), \quad (15)$$

$$I_2 = \int_q \frac{q^{a-d}}{(q^2 + \hat{m}^2)^2} = K_4 \frac{\hat{m}^{-\delta}}{\delta} + \mathcal{O}(1), \quad (16)$$

$$I_3 = \int_q \frac{q^{2(a-d)}}{(q^2 + \hat{m}^2)^2} = \frac{K_4 \hat{m}^{-2\delta+\varepsilon}}{2\delta - \varepsilon} + \mathcal{O}(1), \quad (17)$$

where we have set $\hat{m} = m/\sqrt{c_0}$ and K_d is the area of a d -dimensional sphere divided by $(2\pi)^d$. Let us define the renormalized dimensionless disorder R_i as

$$m^\varepsilon R_1(u) = R_{10}(u) + \delta^1 R_1(u), \quad (18)$$

$$m^\delta R_2(u) = R_{20}(u) + \delta^1 R_2(u). \quad (19)$$

Note that to one-loop order, there is no correction due to the renormalization of elasticity (see below). The β

functions are defined as the derivative of $R_i(u)$ with respect to the mass m at fixed bare disorder $R_{i0}(u)$. It is convenient to rescale the field u by m^ζ and write the β functions for the function $\tilde{R}_i = K_4 m^{-4\zeta} R_i(u m^\zeta)$. Dropping the tilde subscript, the flow equations to one-loop order read

$$\begin{aligned} \partial_\ell R_1(u) &= (\varepsilon - 4\zeta)R_1(u) + \zeta u R_1'(u) \\ &\quad + \frac{1}{2}[R_1''(u) + R_2''(u)]^2 + A R_1''(u), \end{aligned} \quad (20)$$

$$\partial_\ell R_2(u) = (\delta - 4\zeta)R_2(u) + \zeta u R_2'(u) + A R_2''(u), \quad (21)$$

where $A = -[R_1''(0) + R_2''(0)]$ and $\partial_\ell := -m \frac{\partial}{\partial m}$. The FPs of flow equations (20) and (21) characterizing different universality classes have been computed numerically in Ref. 35 and the corresponding critical exponents have been derived to first order in ε and δ . The remarkable property of the FRG flow is that the LR part of disorder correlator $R_2(u)$ remains an analytic function along the flow for all universality classes. We will show below that due to this feature, one can obtain the critical exponents to two-loop order just computing the two-loop correction to elasticity and avoiding exhaustive two-loop calculations.

C. Correction to elasticity

The STS violation causes a renormalization of elasticity. The first order correction to the single-replica part of effective action is expressed by the following diagram:

$$\begin{aligned} \text{Diagram} &= - \int_{x,x'} \sum_a \frac{R_{20}''(u_x^a - u_{x'}^a) g(x-x')}{2T} C(x-x'), \end{aligned} \quad (22)$$

where the bare correlation function $C(x)$ is given by Eq. (9). Using the short distance expansion

$$u_x^a - u_{x'}^a = \sum_{i=1}^d (x_i - x'_i) \frac{\partial u_x^a}{\partial x_i} + \dots \quad (23)$$

and identifying the terms of the kind $-(\nabla u_x^a)^2/2T$ as a correction to elasticity, we find

$$\begin{aligned} \delta^1 c &= \frac{1}{2d} R_{20}^{(4)}(0) \int_x x^2 g(x) C(x) \\ &= c_0 R_{20}^{(4)}(0) \frac{\delta - \varepsilon}{4\delta} \hat{m}^{-\delta} + O(\varepsilon, \delta), \end{aligned} \quad (24)$$

where in the last line we have included K_4/c_0^2 in a redefinition of $R_{20}(u)$. Since Eq. (24) is finite for $\varepsilon, \delta \rightarrow 0$, the elasticity does not get corrected to one-loop order.

We now turn to the two-loop corrections. The three different sets of diagrams contributing to elasticity are depicted in Fig. 3. The details of calculations are given in the Appendix. Summing up all contributions, we arrive

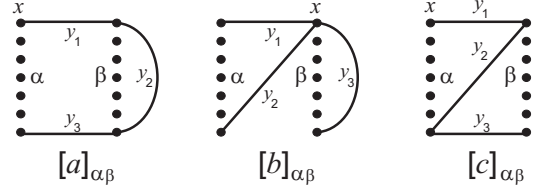


FIG. 3: Single-replica two-loop diagrams correcting elasticity. The dotted line corresponds to either SR disorder vertex ($\alpha, \beta = 1$) or to LR disorder vertex ($\alpha, \beta = 2$). The solid line corresponds to bare correlation functions $C(y)$. The corresponding expressions are computed in the Appendix.

at

$$\begin{aligned} \frac{\delta^2 c}{c_0} &= R_{10}''(0) R_{20}^{(6)}(0) \hat{m}^{-(\varepsilon+\delta)} \frac{\varepsilon - \delta}{\varepsilon + \delta} \frac{1}{4\varepsilon} \\ &\quad + R_{20}''(0) R_{20}^{(6)}(0) \hat{m}^{-2\delta} \frac{\varepsilon - \delta}{8\delta^2} + O(1). \end{aligned} \quad (25)$$

To render the poles in ε and δ , we introduce the renormalization group Z factor as follows:

$$c = Z_c [R_1, R_2]^{-1} c_0. \quad (26)$$

The exponent ψ is given then by

$$\psi = -m \frac{d}{dm} \ln Z_c [R_1, R_2] \Big|_0, \quad (27)$$

where subscript 0 indicates a derivative at constant bare parameters. Taking the derivative with respect to the mass, we obtain

$$\begin{aligned} -m \frac{d}{dm} \ln Z_c \Big|_0 &= -\frac{1}{4} R_{20}^{(4)}(0) (\delta - \varepsilon) \hat{m}^{-\delta} \\ &\quad + R_{10}''(0) R_{20}^{(6)}(0) \hat{m}^{-(\varepsilon+\delta)} \frac{\delta - \varepsilon}{4\varepsilon} \\ &\quad + R_{20}''(0) R_{20}^{(6)}(0) \hat{m}^{-2\delta} \frac{\delta - \varepsilon}{4\delta}. \end{aligned} \quad (28)$$

To calculate ψ , we have to express the bare disorder via renormalized one as follows:

$$\begin{aligned} R_{20}^{(4)}(0) &= m^\delta \left[R_2^{(4)}(0) + R_1''(0) R_2^{(6)}(0) \frac{1}{\varepsilon} \right. \\ &\quad \left. + R_2''(0) R_2^{(6)}(0) \frac{1}{\delta} \right]. \end{aligned} \quad (29)$$

Substituting Eq. (29) in Eq. (28), we find that the leading two-loop corrections are exactly canceled by the counterterms, so that we leave with

$$\psi = -\frac{1}{4} (\delta - \varepsilon) R_2^{(4)}(0). \quad (30)$$

The finite part of the single-replica two-loop diagrams (25) is expected to correct elasticity at three-loop order. Hence, we argue that the perturbation theory for this

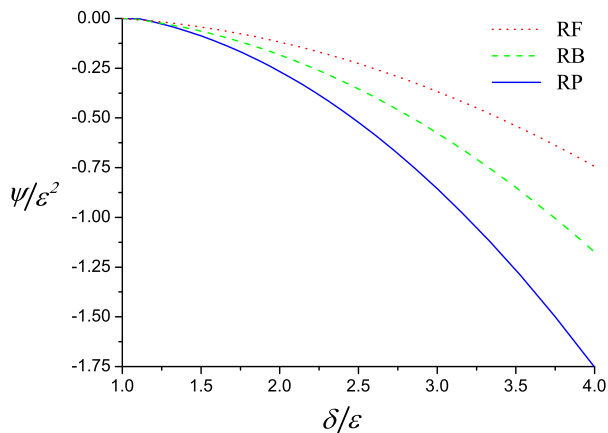


FIG. 4: (Color online) Exponent ψ as a function of δ/ε at two-loop order for the RF, RB, and RP universality classes.

model is organized in such a way that the single-replica p -loop diagrams correct the elasticity only to $(p+1)$ order. Since $R_2(u)$ remains analytic along the FRG flow, we have $R_2^{(4)}(0) > 0$, and therefore, $\psi < 0$. The corresponding values of the exponent ψ computed for the RF, RB, and RP universality classes using the FPs found in Ref. 35 are shown in Fig. 4.

D. Roughness exponent to two-loop order

We now show how one can calculate the roughness exponent ζ to second order in ε and δ knowing only the exponent ψ computed to second order in Sec. III C. To that end, we do not need the whole FRG to two-loop order. Let us start with the RB universality class. The roughness exponent is fixed by a stable RB FP solution of Eqs. (20) and (21) which decays exponentially fast for large u . The equations possess both the SR RB FP with $R_2(u) = 0$ and the LR RB FP with $R_2(u) \neq 0$. The roughness exponent corresponding to the SR RB FP is known to second order in ε and reads^{22,24}

$$\zeta_{\text{SRRB}} = 0.208298\varepsilon + 0.006858\varepsilon^2 + O(\varepsilon^3). \quad (31)$$

Despite the smallness of the two-loop correction, the estimation of the exponent in $d=1$, $\zeta_{\text{SRRB}} = 0.6866$ given by Eq. (31), visibly differs from the known exact result $2/3$. One can improve the accuracy of ζ by use the Padé approximant $[2/1]$ involving also the unknown third order correction. Tuning the latter in order to reproduce the exact result $2/3$ for $\varepsilon = 3$, we end up with the expression

$$\zeta_{\text{SRRB}}^{\text{imp}} = \frac{0.208298\varepsilon + 0.040017\varepsilon^2}{1 + 0.159192\varepsilon}, \quad (32)$$

which is expected to be fairly accurate for $0 \leq \varepsilon \leq 3$.

We now focus on the LR RB FP with $R_2(u) \neq 0$. We can integrate both sides of flow equation (21) over u from 0 to ∞ taking into account that for RB disorder

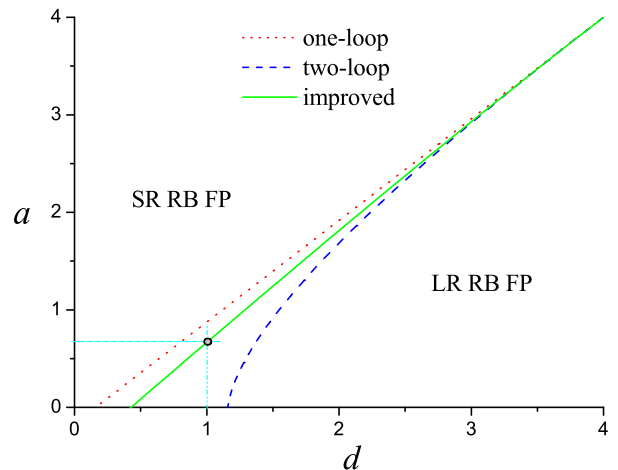


FIG. 5: (Color online) Stability regions of SR and LR RB FPs on plane (d, a) . The borderline between regions is given by equation $\zeta_{\text{LRRB}} = \zeta_{\text{SRRB}}$ (on the exact crossover line also $\psi = 0$). The shown lines are computed using the one-loop, two-loop, and improved results. The circle is a point on the exact crossover line.

$R_2(u)$ decays exponentially fast. Since for RB disorder the integral $\int_0^\infty du R_2(u)$ is nonzero, we can determine the roughness exponent $\zeta_{\text{LRRB}} = \delta/5$ to first order in ε and δ . Fortunately, one can go beyond the one-loop approximation. Indeed, the direct inspection of diagrams contributing to the flow equation (21) shows that the higher orders can only be linear in even derivatives of $R_2(u)$. The only term which is linear in $R_2(u)$ comes from the renormalization of elasticity and can be rewritten as $2\psi R_2(u)$ to all orders. Hence, we have to all orders

$$\partial_\ell \int_0^\infty du R_2(u) = (\delta - 5\zeta + 2\psi) \int_0^\infty du R_2(u), \quad (33)$$

and as a consequence, $\int_0^\infty du R_2(u)$ is exactly preserved along the FRG flow resulting in the exact identity

$$\zeta_{\text{LRRB}} = \frac{\delta + 2\psi}{5}. \quad (34)$$

Substituting Eq. (30) into Eq. (34), we obtain the roughness exponent ζ_{LRRB} to second order in ε and δ . Before we proceed to compute the exponents, let us to check stability of the SR and LR RB FPs. As was shown in Ref. 35, the SR RB FP is unstable with respect to LR disorder if $\zeta_{\text{LRRB}} > \zeta_{\text{SRRB}}$. To one-loop order, this gives that the SR RB FP is stable for $\delta < 1.0415\varepsilon$. Equating (34) and (32), we can compute the stability regions to second order in ε and δ (see Fig. 5). The alternative way to determine the crossover line relies on the requirement that the exponent ψ is a continuous function of ε and δ . It is zero in the region controlled by the SR FP, and therefore has to vanish when approaching the crossover line from the LR stability region. Since the ψ is of second order in ε and δ , the ψ criterion at two-loop order

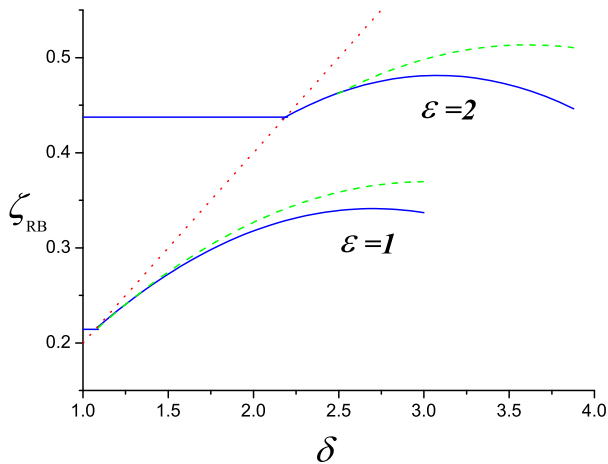


FIG. 6: (Color online) RB disorder: roughness exponent as a function of δ for $\varepsilon = 1$ and $\varepsilon = 2$. The solid lines are computed using the improved estimation (35) and (36) of the exponent ψ . The dashed lines are computed using ψ which is given by Eq. (30) and shown in Fig. 4. The dotted line is the one-loop result $\zeta_{\text{LRRB}} = \delta/5$ which does not depend on ε .

gives the same stability regions as the roughness exponents equating at one-loop order. However, we can significantly improve the latter if we take into account that $\psi = 0$ on the crossover line. The resulting crossover line is shown in Fig. 5. We can also improve the two-loop estimation of ψ . To that end, we write down a formal expansion of ψ in ε ,

$$\psi = \varepsilon^2 f_1(\delta/\varepsilon) + \varepsilon^3 f_2(\delta/\varepsilon) + \dots \quad (35)$$

The function $f_1(x)$ is basically the function shown in Fig. 4. We now tune the function $f_2(x)$ in order to make $\psi = 0$ on the crossover line and find

$$f_2(x) = \frac{0.159192x - 0.200087}{x - 1.04149} f_1(x). \quad (36)$$

Using Eqs. (35) and (36), we compute the roughness exponent ζ_{LRRB} as a function of δ for $\varepsilon = 1$ and $\varepsilon = 2$ (see Fig. 6). Unfortunately, the accuracy rapidly decays with ε , so that estimation of the roughness exponent for $\varepsilon = 3$ is very difficult and postponed to Sec. V.

Similar to the case of RB disorder, one can show that the roughness exponent at the LR RF FP is exactly given by

$$\zeta_{\text{LRRF}} = \frac{\delta + 2\psi}{3}, \quad (37)$$

and the crossover line between the SR and LR RF FPs is exactly given by $\delta = \varepsilon$.

IV. RESPONSE TO TILT

In this section, we study the response of a d -dimensional elastic object to a small tilting force tending

to rotate the object in the plane (x_1, u) . The tilting force can be incorporated into the Hamiltonian as follows:

$$\mathcal{H}_h[u] = \mathcal{H}[u] - h \int d^d x \partial_{x_1} u_x. \quad (38)$$

Such a force can be caused, for example, by a tilt of the applied field in superconductors or by tilted boundary conditions in the case of interfaces. For superconductors, we have $h = \phi_0 H_\perp / (4\pi)$, where H_\perp is the component of the applied magnetic field transverse to the flux lines directed along x_1 and ϕ_0 is the magnetic flux quantum.¹² Since we restrict our consideration to the case $N = 1$, our results can be applied only to flux lines confined in $(1+1)$ dimensions. However, the methods we use here can be extended to general N , and therefore applied to vortices in $(2+1)$ dimensions.

We focus on the response of the system to a small field h , which can be measured by the average angle between the perturbed and unperturbed orientations of the object in the (x_1, u) plane: $\vartheta(h) := \overline{\partial_{x_1} u_x}$. In the absence of disorder the straightforward minimization of the Hamiltonian leads to the linear response: $\vartheta(h) = h/c$. To study the effect of disorder, it proves more convenient to work in the tilted frame: $u_x \rightarrow u_x + \vartheta x_1$. The corresponding Hamiltonian is

$$\mathcal{H}_h[u] = \int d^d x \left[\frac{1}{2} \sum_{i=1}^d c_i (\partial_{x_i} u_x)^2 + V(x, u_x + \vartheta x_1) - (h - c_1 \vartheta) \partial_{x_1} u_x \right], \quad (39)$$

where the field u satisfies $\overline{\partial_{x_1} u_x} = 0$. Note that due to the violation of the STS symmetry, the tilted system can exhibit anisotropic effective elasticity even if the bare elasticity and disorder are isotropic. We now show by simple power counting that a finite tilt does introduce a new length scale in the problem which can be associated with the correlation length defined through the connected two point correlator,

$$\Omega(x; \vartheta) = \overline{\partial_{x_1} u(0) \partial_{x_1} u(x)}^c \sim \exp(-x_1/\xi_\vartheta). \quad (40)$$

Indeed, upon scaling transformation $x \rightarrow bx$, $u \rightarrow b^\zeta u$ the arguments of the disorder term in Hamiltonian (39) scale like $V(bx, b^\zeta u_x + \vartheta bx_1)$. Comparing two terms of the last argument, we find that finite ϑ changes the character of disorder correlator above the length scale

$$\xi_\vartheta \sim \vartheta^{-1/(1-\zeta)}, \quad (41)$$

diverging for $\vartheta \rightarrow 0$ provided that $\zeta < 1$. Below ξ_ϑ one can neglect the tilt, while above ξ_ϑ the dependence on u_x is completely washed out and the ϑ term starts to suppress the correlation of disorder along x_1 . Thus, ξ_ϑ serves as the correlation length along x_1 , and therefore c_1 does not get renormalized beyond this scale. In the next two sections, we investigate the difference in the response to tilt for anisotropically distributed extended defects and isotropic LR-correlated disorder.

A. Response in the presence of columnar disorder

Here, we extend the previous one-loop FRG studies^{32,34} of elastic systems in the presence of columnar disorder to two-loop order and proceed to describe the transverse Meissner physics in a quantitative way. We consider the model with ε_d -dimensional extended defects introduced in Sec. II A. We take $c_i = c_{\parallel}$ ($i = 1, \dots, \varepsilon_d$) and we are also free to put $c_i = 1$ ($i = \varepsilon_d + 1, \dots, d$) since they do not get corrected by disorder. Simple power counting shows that the upper critical dimension of the problem is $d_{\text{uc}} = 4 + \varepsilon_d$. We use the dimensional regularization of integrals with a $\tilde{\varepsilon} = 4 - d + \varepsilon_d$ expansion. The FRG flow equations to two-loop order read

$$\begin{aligned} \partial_\ell R(u) &= (\tilde{\varepsilon} - 4\zeta)R(u) + \zeta u R'(u) - TR^{(4)}(u) \\ &\quad + \frac{1}{2}R''(u)^2 - R''(0)R''(u) - \frac{1}{2}R'''(0^+)^2 R''(u) \\ &\quad + \frac{1}{2}(R''(u) - R''(0))R'''(u)^2, \end{aligned} \quad (42)$$

$$\partial_\ell \ln c_{\parallel} = R^{(4)}(0) + R^{(4)}(0)^2 + 2R'''(0)R^{(5)}(0), \quad (43)$$

$$\partial_\ell \ln T = -\theta_T - \frac{\varepsilon_d}{2}R^{(4)}(0) + O(R^2), \quad (44)$$

$$\partial_\ell \tilde{h} = c_{\parallel}^{1/2} \Lambda_0 e^{-\ell} R'''(0^+) + O(R^2). \quad (45)$$

where $\theta_T = d - 2 + 2\zeta$ and Λ_0 is the bare cutoff. In Eq. (45), \tilde{h} is the coefficient in front of the term

$$\tilde{h} \sum_a \int d^d x |\nabla_{\parallel} u_x^a| \quad (46)$$

ultimately generated in the effective Hamiltonian along the FRG flow.³² The correction to \tilde{h} is strongly UV diverging, and thus is nonuniversal. Note that the flow equation for the generalized columnar disorder (42) coincides to all orders with that for pointlike disorder up to change $\tilde{\varepsilon} \rightarrow \varepsilon$.

Let us start from the analysis at $T = 0$. The flow picture very resembles that for the depinning transition with tilt ϑ , longitudinal elasticity c_{\parallel} , and tilting field h playing the roles of velocity, friction, and driving force, respectively. For $d < 4 + \varepsilon_d$, the running disorder correlator $R^{(4)}(u)$ blows up at the Larkin scale

$$l_c = \frac{1}{\tilde{\varepsilon}} \ln \left(1 + \frac{\tilde{\varepsilon}}{3|R_0^{(4)}(0)|} \right). \quad (47)$$

Consequently, the longitudinal elasticity diverges at zero tilt ϑ in a way similar to mobility divergence at the depinning transition in quasistatic limit. Beyond the Larkin scale $l > l_c$, the $R^{(2)}(u)$ develops a cusp at origin, $R'''(0^+) > 0$. The term (46) is generated in the effective Hamiltonian and the $R^{(4)}(0)$ changes its sign from positive to negative. The latter leads to a power law decay of the longitudinal elasticity $c_{\parallel} \propto L^{-\psi}$ with

$$\psi = -R^{*(4)}(0) - R^{*(4)}(0)^2 - 2R^{*''''}(0)R^{*(5)}(0), \quad (48)$$

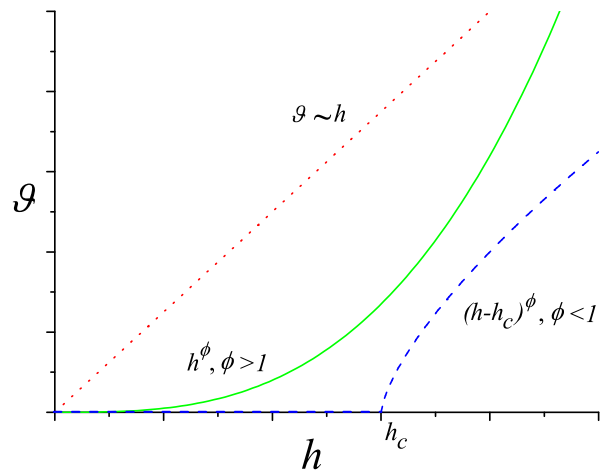


FIG. 7: (Color online) Schematic plot of the elastic object response to a transverse field for uncorrelated disorder (dotted line), columnar disorder (dashed line), and LR-correlated disorder (solid line).

where $R^*(u)$ is a FP solution of the flow equation (42). Similar to the threshold force generation at the depinning transition, term (46) reduces the tilting force and generates the critical tilting force h_c . The flow equation (45) allows us to estimate the nonuniversal value of h_c . Integrating Eq. (45) up to large scales, we find

$$h_c = \frac{c_0^{1/2} \Lambda_0 e^{-l_c(1+\psi/2)}}{1 + \psi/2} R^{*''''}(0^+). \quad (49)$$

We now in a position to compute the exponent ϕ , which we define as

$$\vartheta \propto (h - h_c)^\phi. \quad (50)$$

To that end, we renormalize the equilibrium balance equation $h - h_c = c_1(L)\vartheta$ up to the scale $L = \xi_\vartheta$ at which the elasticity c_1 stops to get renormalized. Using Eq. (41), we obtain the exact scaling relation

$$\phi = \left(1 + \frac{\psi}{1 - \zeta} \right)^{-1}. \quad (51)$$

The exponents ζ , ψ , and ϕ computed to second order in $\tilde{\varepsilon}$ for different universality classes are summarized in Tab. I. Note that expansions in $\tilde{\varepsilon}$ are expected to be Borel nonsummable, and thus ill behaved for high orders and large $\tilde{\varepsilon}$. In this light, the using of exact relation (51) may be more favorable than the expansions given in the last column of Table I. Systems described by the RP universality class exhibit slow logarithmic growth of displacements

$$\overline{(\bar{u}_{x_\perp} - \bar{u}_0)^2} = \mathcal{A}_d \ln x_\perp, \quad (52)$$

where $\bar{u}_{x_\perp} := L^{-\varepsilon_d} \int d^{\varepsilon_d} x_{\parallel} u_x$. The universal amplitude can be easily deduced from the results for the uncorrelated disorder and to two loop reads

$$\mathcal{A}_d = \frac{\tilde{\varepsilon}}{18} + \frac{\tilde{\varepsilon}^2}{108} + O(\tilde{\varepsilon}^3), \quad (53)$$

TABLE I: Critical exponents for elastic systems with generalized columnar disorder computed to two-loop order.

	ζ	ψ	ϕ
RP	0	$\frac{1}{3}\tilde{\varepsilon} + \frac{1}{9}\tilde{\varepsilon}^2$	$1 - \frac{1}{3}\tilde{\varepsilon} + O(\tilde{\varepsilon}^3)$
RF	$\frac{1}{3}\tilde{\varepsilon}$	$\frac{2}{9}\tilde{\varepsilon} + \frac{5}{162}\tilde{\varepsilon}^2$	$1 - \frac{2}{9}\tilde{\varepsilon} - \frac{1}{18}\tilde{\varepsilon}^2$
RB	$0.208298\tilde{\varepsilon}$ $+ 0.006858\tilde{\varepsilon}^2$	$0.263902\tilde{\varepsilon}$ $+ 0.053615\tilde{\varepsilon}^2$	$1 - 0.263902\tilde{\varepsilon}$ $- 0.038941\tilde{\varepsilon}^2$

where we have fixed the period to 1. The logarithmic growth of displacements corresponds to a slow power-law decay of the translation order, and thus should lead to Bragg peaks unexpected for a strongly pinned Bose-glass. The system under consideration shares features of the Bragg glass, such as power-law decay of the translation order, and the strong Bose glass, namely, the diverging tilt modulus (transverse Meissner effect). One can expect this behavior for a weak Bose-glass which is pinned collectively. Recently, such a glassy phase called Bragg-Bose glass was observed in numerical simulations of vortices in bulk superconductor at low concentrations of columnar disorder and low temperatures.^{44,45}

A finite temperature $T > 0$ rounds the cusp of the running disorder correlator $R_l(u)$, so that in the boundary layer $u \sim T_l$, it significantly deviates from the FP solution and obeys the following scaling form:⁴⁶

$$R_l''(u) = R_l''(0) - T_l \left[1 - \sqrt{1 + (u\chi/T_l)^2} \right], \quad (54)$$

where $\chi = |R^{*''}(0)|$. However, as was pointed in Ref. 33 the flow equations for columnar disorder have a remarkable feature in comparison with uncorrelated disorder. Indeed, substituting the boundary layer scaling (54) in the temperature flow equation (44), we obtain

$$\partial_l T_l = -\theta_T T_l - \varepsilon_d \chi^2 / 2. \quad (55)$$

As follows from Eq. (55), the effective temperature T_l vanishes at a finite length scale $L_{\text{loc}} = e^{l_{\text{loc}}}/\Lambda_0$,

$$l_{\text{loc}} = \frac{1}{\theta_T} \ln \left(1 + \frac{2\theta_T T_0}{\varepsilon_d \chi^2} \right), \quad (56)$$

so that the localization effects are settled only on scales larger than $l_{\text{loc}} > l_c$.

B. Interacting disordered bosons in (1+1) dimensions

Let us discuss the special case of flux lines in (1+1) dimensions which the qualitative phase diagram is shown in Fig. 1. The transverse Meissner physics for collectively pinned weak Bose glass and small tilt angles $\vartheta = B_{\perp}/B_{\parallel}$ can be explored using the results obtained in the previous section for the RP universality class with $\tilde{\varepsilon} = 4 - 2 + 1 = 3$.

Here, we restore the dependence on the flux line density n_0 fixing the period of $R(u)$ to $1/n_0$. In contrast to the Bragg-glass, the weak Bose-glass survives in $d = 2$. Indeed, for uncorrelated disorder in $d = 2$, the temperature turns out to be marginally relevant, so that the system has a line of FPs describing a super-rough phase with anomalous growth of the two-point correlation $(u_x - u_0)^2 = A(T) \ln^2 x + O(\ln x)$.⁴⁷ According to Eqs. (55) and (56) for columnar disorder the temperature vanishes at finite, though a very large scale

$$l_{\text{loc}} = \frac{2T_0}{n_0^2 \chi^2}. \quad (57)$$

Unfortunately, the large value of $\tilde{\varepsilon}$ makes estimation of ϕ extremely unreliable. Indeed, the expansion in $\tilde{\varepsilon}$ shown in Table I leads to a zero value of ϕ . The exact scaling relation (51) with ψ computed using the expression from Table I gives

$$\begin{aligned} \phi(1+1) &= \frac{1}{2} \quad (\text{one loop}), \\ \phi(1+1) &= \frac{1}{3} \quad (\text{two loop}). \end{aligned} \quad (58)$$

The one-loop result reproduces the estimation $\phi = 1/2$ given by heuristic random walk arguments based on the entropy of flux lines wandering in the presence of thermal fluctuations.¹² The model of vortices wandering in a random array of columnar defects can be mapped onto a quantum problem of disordered bosons.⁹ One can regard each vortex as an imaginary time world line of a boson, so that the columnar pins parallel to vortices become quenched pointlike disorder in the quantum problem. The transverse magnetic field H_{\perp} will play the role of an imaginary vector potential h for the bosons,⁴⁸ so that the bosonic Hamiltonian turns out to be non-Hermitian:

$$\begin{aligned} \hat{\mathcal{H}} &= -\frac{\hbar^2}{2m} \int dx \psi^{\dagger}(x) (\partial_x - h)^2 \psi(x) + \int dx V(x) \hat{n}(x) \\ &+ \frac{1}{2} \int dx dx' \hat{n}(x) U(x - x') \hat{n}(x'). \end{aligned} \quad (59)$$

Here, $\psi^{\dagger}(x)$, $\psi(x)$ are the bosonic creation and annihilation operators, and $\hat{n}(x) = \psi^{\dagger}(x)\psi(x)$ is the density operator. $U(x)$ is a short-range repulsive interaction potential between bosons with the strength $U_0 = \int dx U(x)$. The disorder is described by a time-independent Gaussian random potential $V(x)$ with zero mean $\overline{V(x)} = 0$ and short-range correlations $\overline{V(x)V(x')} = V_0 \delta(x - x')$. We can pass to a quantum hydrodynamic formulation of model (59) expressing everything through the bosonic fields $\theta(x)$ and $\varphi(x)$ which satisfy the canonical commutation relation⁴⁹

$$[\partial_x \varphi(x), \theta(x')] = -i\delta(x - x'). \quad (60)$$

For bosons with average density n_0 , this gives

$$\hat{\mathcal{H}} = \frac{v_p \hbar}{2} \int dx \left[\frac{g}{\pi} (\partial_x \varphi(x) - i\hbar)^2 + \frac{\pi}{g} (\partial_x \theta(x))^2 \right] + n_0 \int dx V(x) \sum_{p=-\infty}^{\infty} e^{2\pi i p (n_0 x + \theta(x))}, \quad (61)$$

where in the disorder part we have retained only the leading contributions coming from the backscattering on impurities. The forward scattering term can be eliminated by a shift of the phonon field $\theta(x)$ which does not depend on the time t , and thus, this term does not contribute to the current $J \sim \partial_t \theta(x)$. The Luttinger liquid parameter g and the phonon velocity v_p are given by

$$g^2 = \frac{\pi^2 n_0 \hbar^2}{m U_0}, \quad v_p^2 = \frac{U_0 n_0}{m}. \quad (62)$$

The imaginary time ($\tau = it$) action corresponding to Hamiltonian (61) for a particular distribution of disorder can be derived using the canonical transformation

$$\mathcal{S}_V = \int dx d\tau [\mathcal{H} - i\Pi_\theta(x) \partial_\tau \theta(x)]. \quad (63)$$

Here, $\partial_\tau \theta(x) = (i/\hbar)[H, \theta(x)] = -igc\Pi_\theta(x)/(\pi\hbar)$ and $\Pi_\theta = \hbar \partial_x \varphi(x)$ is the momentum conjugate to $\theta(x)$ which is given by Eq.(60). Averaging $e^{-S_V/\hbar}$ over disorder by means of the replica trick and keeping only the most relevant terms, we obtain the replicated action

$$\begin{aligned} \mathcal{S} = & \sum_a \int dx d\tau \left\{ \frac{\pi \hbar}{2g} \left[\frac{1}{v_p} (\partial_\tau \theta_a(x, \tau))^2 \right. \right. \\ & \left. \left. + v_p (\partial_x \theta_a(x, \tau))^2 \right] + \hbar \partial_\tau \theta_a(x, \tau) \right\} - \frac{V_0 n_0^2}{\hbar} \\ & \times \sum_{ab} \int dx d\tau d\tau' \cos \{2\pi [\theta_a(x, \tau) - \theta_b(x, \tau')]\}. \quad (64) \end{aligned}$$

The imaginary time action (64) is identical to the Hamiltonian of periodic elastic system with columnar disorder (6). The imaginary time plays the role of the longitudinal coordinate $\tau \longleftrightarrow x_{\parallel}$ which is parallel to columnar pins. The Planck constant stands for the temperature $\hbar \longleftrightarrow T$, and the phonons are related to the dimensionless displacements field $\theta(x, \tau) = -n_0 u(x)$. There is the following correspondence between quantities in the vortices and bosons problems⁴⁸

$$g = \frac{\pi T n_0^2}{\sqrt{c_{\parallel} c_{\perp}}}, \quad v_p = \sqrt{c_{\perp}/c_{\parallel}}. \quad (65)$$

The vortex tilt angle ϑ caused by the transverse field H_{\perp} corresponds to the boson current $J = (-i)\partial\mathcal{H}/\partial h$ induced by the imaginary vector potential h . For $h = 0$, the disordered bosons undergoes a superfluid-insulator transition at $g = 3/2$. This determines the temperature T_{BG} , such that $g(T_{\text{BG}}) = 3/2$, above which vortices form a liquid (see Fig. 1). It is known that in one dimension

there is no difference between bosons and fermions, and both types of particles are described by the Luttinger liquid (61). In particular, the hard-core bosons can be mapped onto free fermions that corresponds to a special value of the Luttinger parameter $g(T^*) = 1$, which defines the temperature T^* . In Ref. 14, the mapping onto free fermions was used to study the transverse Meissner effect in (1+1) dimensions. The free fermions on a lattice is described by the tight-binding model,

$$\hat{\mathcal{H}} = \sum_i \left[-w_i (c_i^\dagger c_{i+1} e^{-h} + c_{i+1}^\dagger c_i e^h) + (\epsilon_i - \mu) c_i^\dagger c_i \right], \quad (66)$$

where c^\dagger, c are on site fermion creation and annihilation operators, and μ is the chemical potential. w_i is a random hopping matrix element and ϵ_i is a random pinning energy. In Ref. 14, both cases, the random pinning and the random hopping models, were studied using the exact results for the Lloyd model and the strong-randomness real-space RG, respectively. It was found in both cases that $J \sim h - h_c$, i.e., $\phi = 1$, that significantly differs from the FRG prediction (58). The difference can be attributed to that the free fermions analog is limited to a special point $g = 1$ ($T = T^*$), while the FRG prediction may be valid only for low temperatures since it is controlled by the zero-temperature fixed point. The correspondence between the temperature and the Planck constant in both problems reflects that the zero-temperature FRG FP may have a counterpart in the quantum problem in the form of an instanton solution. This may account for the consistency of the exponent ϕ computed by FRG and estimated using heuristic arguments of kink statistics.

The high- T_c superconductor films grown by deposition often exhibit larger critical currents than their bulk counterparts due to the formation of dislocations running parallel to the crystalline axis, and thus, they are natural candidates to verify the above results. However, as was discussed in Ref. 50, the picture may be more involved since the dislocation lines can meander or they can be of relatively short length that breaks up the Bose glass into pieces along the direction of the crystalline axis.

C. Response in the presence of long-range correlated disorder

We now consider the response to tilt in the presence of isotropic LR-correlated disorder. In contrast to the case of generalized columnar disorder the \tilde{h} term is not generated due to the analyticity of the LR part $R_2(u)$ of disorder correlator. Moreover, the elasticity remains finite along the FRG flow though it grows as a power law $c \sim L^{-\psi}$ with $\psi < 0$ given by Eq. (30) and shown in Fig. 4. As a consequence, there is no threshold transverse field: the systems is tilted for any finite tilting force. Renormalizing the balance equation $h = c_1 \vartheta$ up to the

scale ξ_θ given by Eq. (41), we see that the response to the tilting force h is given by a power law

$$\vartheta(h) \sim h^\phi, \quad (67)$$

with the exponent $\phi > 1$ defined by Eq.(51). The response to tilt in systems with uncorrelated, columnar and LR-correlated disorders is shown in Fig. 7. As one can see from the figure, the response of systems with LR-correlated disorder interpolates between the response of systems with uncorrelated and columnar disorder. In particular, we argue that in the presence of LR-correlated disorder, vortices can form a new vortex glass phase which exhibits Bragg peaks and vanishing linear tilt modulus without transverse Meissner effect. We will refer to this phase as the strong Bragg glass.

In analogy with the Bose glass, one can attempt to map the system with linear defects of random orientation corresponding to LR-correlated disorder with $a = d - 1$ to a quantum system consisting of interacting bosons and heavy particles moving with random quenched velocities according to classical mechanics.

V. KARDAR-PARISI-ZHANG EQUATION WITH TEMPORALLY CORRELATED NOISE

In this section, we address the relevance of our results to the Kardar-Parisi-Zhang (KPZ) equation (and closely related Burgers equation), which describes the dynamics of a stochastically growing interface.⁵¹ The latter is characterized by a height function $h(x, t)$, $x \in \mathbb{R}^d$ which obeys the nonlinear stochastic equation of motion

$$\partial_t h = \nu \nabla^2 h + \frac{\lambda}{2} (\nabla h)^2 + \eta(x, t). \quad (68)$$

The first term in Eq. (68) represents the surface tension, while the second term describes tendency of the surface locally grow to normal itself. The stochastic noise $\eta(x, t)$ is usually assumed to be Gaussian with short-range correlations. Here, we consider the noise with long-range correlations in both time and space. It is defined in Fourier by⁵²

$$\langle \eta(k, \omega) \eta(k', \omega') \rangle = 2D(k, \omega) \delta^{d'}(k + k') \delta(\omega + \omega'), \quad (69)$$

with the noise spectral density function having power-law singularities of the form

$$D(k, \omega) = D_0 + D_\theta k^{-2\rho} \omega^{-2\theta}. \quad (70)$$

Such temporal correlations can originate from impurities which do not diffuse and impede the growth of the interface, while the space correlations can be due to the presence of extended defects. Since there is no intrinsic length scale in the problem, asymptotics of various correlation functions are given by simple power laws. For instance, the height-height correlation function scales like

$$\langle [h(x, t) - h(x', t')]^2 \rangle \sim |x - x'|^{2\chi} f\left(\frac{|t - t'|}{|x - x'|^z}\right), \quad (71)$$

where χ is the roughness exponent and z is the dynamic exponent which describes the scaling of the relaxation time with length (do not mix it with the dynamic exponent z at the depinning transition, which is not used in this paper).

Medina *et al.*⁵² studied the KPZ equation with the noise spectrum (70) using the dynamical renormalization group (DRG) approach and here we adopt the notation introduced in their work. Let us briefly outline the results obtained in Ref. 52 restricting ourselves mainly to the case $d' = 1$. The flow equations expressed in terms of dimensionless parameters $U_0 = K_{d'} \lambda^2 D_0 / \nu^3$ and $U_\theta = K_{d'} \lambda^2 D_\theta / \nu^3$ to one loop order read

$$\partial_\ell \ln \nu = z - 2 + \frac{U_0}{4} + \frac{U_\theta}{4} (1 + 2\rho)(1 + 2\theta) \sec(\pi\theta), \quad (72)$$

$$\partial_\ell \ln \lambda = \chi + z - 2 + U_\theta \theta (1 + 2\theta) \sec(\pi\theta), \quad (73)$$

$$\partial_\ell U_\theta = U_\theta [z(1 + 2\theta) - 2\chi - 1 + 2\rho], \quad (74)$$

$$\begin{aligned} \partial_\ell U_0 = & U_0 (z - 2\chi - 1) + \frac{U_0^2}{4} + \frac{U_\theta^2}{2} (1 + 4\theta) \sec(2\pi\theta) \\ & + \frac{1}{2} U_0 U_\theta (1 + 2\theta) \sec(\pi\theta). \end{aligned} \quad (75)$$

Note that the DRG calculations are uncontrolled, in the sense that there is no small parameter. For white noise ($\theta = 0$), the KPZ equation is invariant under tilting of the surface by a small angle. The STS symmetry implies that the vertex λ does not get corrected by the noise to all orders. This results in the exact identity

$$\chi_{\text{SR}} + z_{\text{SR}} = 2. \quad (76)$$

Besides the known SR FP with $U_\theta = 0$, the flow equations (72)-(75) are expected to have a different LR FP with $U_\theta \neq 0$. It was argued that the term U_θ in the noise spectrum $D(k, \omega)$ acquires no fluctuation corrections: the scaling of U_θ is completely determined by its bare dimension so that Eq. (74) is exact to all orders.⁵² This allows one to compute the exact critical value $\theta_c = 1/6$ (for $\rho = 0$) at which there is a crossover from the SR FP to the LR FP. For arbitrary ρ , the crossover to the LR FP happens at

$$6\theta + 4\rho > 1. \quad (77)$$

The term U_θ becomes relevant and as follows from Eq. (74) the exact relation

$$z_{\text{LR}}(1 + 2\theta) - 2\chi_{\text{LR}} + 2\rho = 1 \quad (78)$$

holds at the LR FP. Let us for the moment ignore the noise correction to λ in Eq. (73). This approximation restoring the STS is valid only for small θ and yields

$$z^*(\theta, \rho) = 2 - \frac{1 + 4\theta + 2\rho}{3 + 2\theta}, \quad (79)$$

$$\chi^*(\theta, \rho) = \frac{1 + 4\theta + 2\rho}{3 + 2\theta}. \quad (80)$$

For large θ , one can expect a significant deviation of exponents z and χ from z^* and χ^* . To gain insight into the

problem the authors of Ref. 52 solved the flow equations (72)-(75) for finite θ and $\rho = 0$ numerically. They found that the physical LR FP exists only for $\theta < 1/4$, while nothing special is physically expected at $\theta = 1/4$. It was argued that the problem is originated from infrared divergences of integrals and that infinite number of additional terms generated in the noise spectral density under DRG:

$$D(\omega) = \sum_{n=1}^{\infty} D_n \omega^{-2\theta-(n-1)}. \quad (81)$$

Keeping track of renormalization of all D_n , the authors of Ref. 52 solved the truncated system of flow equations numerically and found that the critical exponents for $\rho = 0$ can be fitted to

$$\chi(\theta) = 1.69\theta + 0.22, \quad (82)$$

$$z(\theta) = \frac{2\chi(\theta) + 1}{1 + 2\theta}. \quad (83)$$

We now revise the problem in the light of what has been learned in the previous sections. Using the well-known Cole-Hopf transformation $Z = \exp[(\lambda/2\nu)h]$ one can eliminate the nonlinear term in Eq. (68) and obtain a diffusion equation in time-dependent random potential

$$\partial_t Z(x, t) = \nu \nabla^2 Z(x, t) + \frac{\lambda}{2\nu} \eta(x, t) Z(x, t). \quad (84)$$

The solution of Eq. (84) can be regarded as the partition function of a directed polymer (DP) of length t in $(d' + 1)$ dimensions with ends fixed at $(0, 0)$ and (x, t) :

$$Z(x, t) = \int_{x(0)=0}^{x(t)=x} Dx(t) \exp \left\{ -\frac{1}{T} \int_0^t dt \left[\frac{c}{2} (\nabla x(t))^2 + \eta(x(t), t) \right] \right\}, \quad (85)$$

with $\nu = T/2c$ and $\lambda = 1/c$. The DP is a one-dimensional ($d = 1, \varepsilon = 3$) elastic object with $d' = N$ - dimensional target space. Thus, the time-dependent noise $\eta(x, t)$ in the KPZ equation is mapped to the quenched disorder V in the DP picture. This gives the exact relation between the dynamic exponent of KPZ problem and the DP roughness exponent which reads

$$z(d') = 1/\zeta(d = 1, N = d'). \quad (86)$$

Spatial correlations in $\eta(x, t)$ corresponds to correlations of quenched disorder V in the directions transverse to the DP. As the exponent ρ varies from 0 to 1, the quenched disorder interpolates between RB and RF universality classes. For example, the exponent z changes from $3/2$ to 1 for $d' = 1$ and white random noise ($\theta = 0$). The stability criterion assures that the LR FP in the FRG picture is stable if $\zeta_{\text{LR}} > \zeta_{\text{SR}}$. This implies that the noise temporal correlations in surface growth problem are relevant only if the corresponding dynamic exponents fulfill the condition $z_{\text{LR}} < z_{\text{SR}}$. Note that this criterion is purely

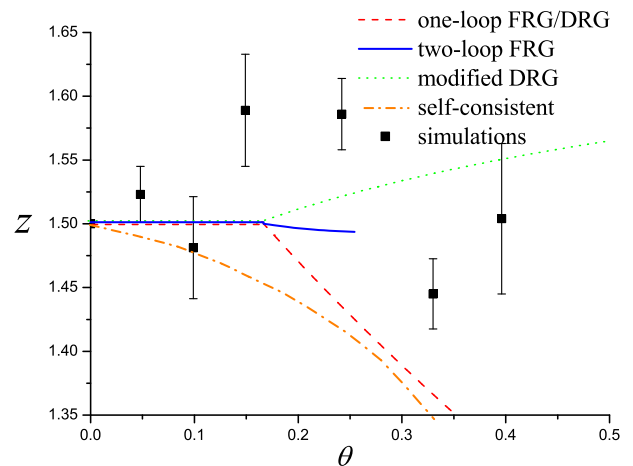


FIG. 8: (Color online) Dynamic exponent z for the KPZ equation ($d' = 1$) with temporally correlated noise ($\rho = 0$) computed using different technique: one-loop FRG/DRG is given by Eq. (79); two-loop FRG is given by Eq. (87) (note that large value $\varepsilon = 3$ does not allow for accurate computation of ψ and z at large θ); modified DRG is given by Eq. (83); self-consistent approximation of Ref. 54 and simulations of Ref. 53.

based on the mapping between the DP and KPZ problems. Since $z_{\text{SR}}(d' = 1, \rho = 0) = 3/2$ the exponent (83) computed using the modified DRG violates the criterion of the LR FP stability, and thus is ruled out. Substituting the roughness exponents computed using FRG for the RB ($\rho = 0$) and RF ($\rho = 1$) universality classes into Eq. (86) and relating $\delta = 3 + 2\theta$, we obtain the exact (for $\rho = 0, 1$ and presumably for any ρ) identity

$$z_{\text{LR}} = \frac{5 - 2\rho}{3 + 2\theta + \psi}. \quad (87)$$

To one-loop order in FRG, i.e., for $\psi = 0$, exponent (87) coincides with the estimation given by DRG (79) for small θ . Though the exponent ψ has been computed in Sec. III C for the RB ($\rho = 0$) and RF ($\rho = 1$) universality classes to two-loop order in a controllable way, the large value $\varepsilon = 3$ of the expansion parameter describing the DP problem makes the estimation of ψ highly unreliable. Nevertheless, since $\psi = 0$ is zero on the crossover line between the LR and SR FPs, we can determine this line exactly for $\rho = 0, 1$ from equation $z_{\text{LR}} < z_{\text{SR}} = 3/2$ that leads back to Eq. (77). Taking into account that ψ is nonpositive for columnar disorder, we obtain the lower and upper bounds on $z(\theta)$ for $\rho = 0$ and $\theta \in [\frac{1}{6}, \frac{1}{2}]$ as

$$\frac{5}{3 + 2\theta} \leq z(\theta) \leq \frac{3}{2}. \quad (88)$$

The critical exponent z computed using FRG, DRG, and measured in numerical simulations of Ref. 53 is shown in Fig. 8. The KPZ equation with temporally correlated noise was also studied using a self-consistent approximation (SCA).⁵⁴ The SCA equations have two strong-

coupling solutions. The first one exhibits a crossover-like behavior at $\theta = \frac{1}{6}$ and corresponds to the one-loop FRG prediction. The second solution, which is considered to be dominant, leads to a smooth dependence of z on θ shown in Fig. 8. Both the SCA solutions are in agreement with the FRG prediction that the exponent z is a decreasing function of θ , while the modified DRG suggests that z increases with θ . However, the second SCA solution considered to be dominant does not satisfy bounds (88), and thus is ruled out.

Let us generalize identity (76) to the case of temporally correlated noise. Note that the solution of the KPZ equation $h(x, t)$ gives the free energy of DP (85). The free energy per unit length $f(\vartheta)$ of the DP tilted by the transverse field H_\perp to the angle ϑ can be written as $f(\vartheta) = f(0) + \tilde{c}\vartheta^\alpha - H_\perp \vartheta$. The naive elastic approximation suggests $\alpha = 2$. In order to take into account the renormalization of elasticity, we determine the exponent α from the condition that at equilibrium the response to the field H_\perp is $\vartheta \sim H_\perp^\phi$. This fixes $\alpha = 1 + 1/\phi$ with ϕ given by Eq. (51). Then the total free energy of the DP of length t can be written as a function of the free end coordinate x as follows:

$$h(x) = tf(0) + tc(x/t)^\alpha - x^\chi. \quad (89)$$

The last term in Eq. (89) describes the typical fluctuation of the free energy due to the disorder and is given by Eq. (71). Balancing the last two terms of Eq. (89) and using Eq. (51), we obtain the exact scaling relation

$$\chi + z = 2 - \psi z, \quad (90)$$

which holds at the LR FP as well as at the SR FP. At the SR FP $\psi = 0$, so that Eq. (90) reduces to the STS identity (76). Excluding ψ from Eqs. (90) and (87), we arrive at the relation (78) valid at the LR FP.

VI. SUMMARY

We have studied the large-scale behavior of elastic systems such as interfaces and lattices pinned by correlated disorder using the functional renormalization group. We consider two types of disorder correlations: columnar disorder generalized to extended defects and LR-correlated disorder. Both types of disorder correlations can be produced in real systems, for example, by subjecting them to either static or rotating ion beam irradiation. We have computed the critical exponents to second order in $\varepsilon = 4 - d$ and $\delta = 4 - a$ for LR-correlated disorder and to second order in $\tilde{\varepsilon} = 4 - \varepsilon + \varepsilon_d$ for ε_d -dimensional extended defects. The correlation of disorder violates the statistical tilt symmetry and results in a highly nonlinear response to a tilt. In the presence of generalized columnar disorder, elastic systems exhibit a transverse Meissner effect: disorder generates the critical field h_c below which there is no response to a tilt and above which the tilt angle behaves as $\vartheta \sim (h - h_c)^\phi$ with a universal exponent $\phi < 1$. The periodic case describes a weak Bose

glass which is expected in type-II superconductors with columnar disorder at small temperatures and at high vortex density which exceeds the density of columnar pins. The weak Bose glass is pinned collectively and shares features of the Bragg glass, such as a power-law decay of translational order, and features of the strong Bose glass, such as a transverse Meissner effect. For isotropic LR-correlated disorder, the linear tilt modulus vanishes at small fields leading to a power-law response $\vartheta \sim h^\phi$ with $\phi > 1$. The response of systems with LR-correlated disorder interpolates between the response of systems with uncorrelated and columnar disorder. We argued that in the presence of LR-correlated disorder vortices can form a strong Bragg glass which exhibits Bragg peaks and a vanishing linear tilt modulus without transverse Meissner effect. The elastic one-dimensional interface, i.e., the directed polymer, in the presence of LR-correlated disorder can be mapped to the Kardar-Parisi-Zhang equation with temporally correlated noise. Using this mapping, we have computed the critical exponents describing the surface growth and compared with the exponents obtained using dynamical renormalization group, self-consistent approximation, and numerical simulations.

Acknowledgments

I would like to thank Kay Wiese, Pierre Le Doussal, Joachim Krug, and David Nelson for inspiring discussions, and the Max Planck Institute for the Physics of Complex Systems in Dresden for hospitality, where part of this work was done. This work has been supported by the European Commission under contract No. MIF1-CT-2005-021897 and partially by the Agence Nationale de la Recherche (05-BLAN-0099-01).

APPENDIX A: CORRECTION TO ELASTICITY: TWO-LOOP DIAGRAMS

In this Appendix, we calculate diagrams shown in Fig. 3 keeping only the terms which correct the elasticity. Here, we set $g_1(x) := \delta^d(x)$ and $g_2(x) := g(x)$. Diagram *a* yields

$$\begin{aligned} [a]_{\alpha\beta} &= -\frac{1}{2T} \int_{y_1, y_2, y_3} R''_\alpha(u_x - u_{x-y_1-y_2-y_3}) \\ &\quad \times R_\beta^{(4)}(u_{x-y_1} - u_{x-y_1-y_2}) g_\alpha(y_1 + y_2 + y_3) \\ &\quad \times g_\beta(y_2) \prod_{l=1}^3 C(y_l), \end{aligned} \quad (A1)$$

where $\alpha, \beta = 1, 2$ and $C(x)$ is given by Eq. (9). Using the short distance expansion (23), we obtain

$$\begin{aligned} [a]_{\alpha\beta}^{(1)} &= -\frac{1}{4dT} (\nabla u_x)^2 R_\alpha^{(4)}(0) R_\beta^{(4)}(0) \int_{\{y\}} \prod_{l=1}^3 C(y_l) \\ &\quad \times (y_1 + y_2 + y_3)^2 g_\alpha(y_1 + y_2 + y_3) g_\beta(y_2) \end{aligned} \quad (A2)$$

and

$$[a]_{\alpha\beta}^{(2)} = -\frac{1}{4dT}(\nabla u_x)^2 R''_{\alpha}(0)R_{\beta}^{(6)}(0) \int_{\{y\}} \prod_{l=1}^3 C(y_l) \times y_2^2 g_{\alpha}(y_1 + y_2 + y_3) g_{\beta}(y_2). \quad (\text{A3})$$

Note that the term $R''_{\alpha}(0)R_{\beta}^{(6)}(0)$ does not contribute since LR disorder $R_2(u)$ remains an analytic function along the FRG flow, while all diagrams with $\alpha = \beta = 1$ are zero due to the STS. We will neglect similar terms in what follows. For diagram b , we have

$$[b]_{\alpha\beta} = \frac{1}{2T} \int_{y_1, y_2, y_3} R''_{\alpha}(u_{x-y_1} - u_{x-y_2}) \times R_{\beta}^{(4)}(u_x - u_{x-y_3}) g_{\alpha}(y_2 - y_1) \times g_{\beta}(y_3) \prod_{l=1}^3 C(y_l). \quad (\text{A4})$$

Applying the short distance expansion (23), we arrive at

$$[b]_{\alpha\beta}^{(1)} = \frac{1}{4dT}(\nabla u_x)^2 R_{\alpha}^{(4)}(0)R_{\beta}^{(4)}(0) \int_{\{y\}} \prod_{l=1}^3 C(y_l) \times (y_1 + y_2)^2 g_{\alpha}(y_1 + y_2) g_{\beta}(y_3) \quad (\text{A5})$$

and

$$[b]_{\alpha\beta}^{(2)} = \frac{1}{4dT}(\nabla u_x)^2 R''_{\alpha}(0)R_{\beta}^{(6)}(0) \int_{\{y\}} \prod_{l=1}^3 C(y_l) \times y_3^2 g_{\alpha}(y_1 + y_2) g_{\beta}(y_3). \quad (\text{A6})$$

Diagram $[c]$ gives

$$[c]_{\alpha\beta} = -\frac{1}{2T} \int_{y_1, y_2, y_3} R'''_{\alpha}(u_x - u_{x-y_1-y_2}) \times R_{\beta}^{(4)}(u_{x-y_1} - u_{x-y_1-y_2-y_3}) g_{\alpha}(y_1 + y_2) \times g_{\beta}(y_2 + y_3) \prod_{l=1}^3 C(y_l). \quad (\text{A7})$$

After short distance expansion, we find that diagrams $[c]$ give rise to elasticity correction only for $\alpha = \beta = 2$ which reads

$$[c]_{\alpha\beta} = -\frac{1}{2dT}(\nabla u_x)^2 R_{\alpha}^{(4)}(0)R_{\beta}^{(4)}(0) \int_{\{y\}} \prod_{l=1}^3 C(y_l) \times [(y_1 + y_2) \cdot (y_2 + y_3)] g_{\alpha}(y_1 + y_2) g_{\beta}(y_2 + y_3). \quad (\text{A8})$$

Straightforward analysis shows that

$$[a]_{1\alpha}^{(1)} = [a]_{\alpha 1}^{(2)} = [b]_{1\alpha}^{(1)} = [b]_{\alpha 1}^{(2)} = 0, \quad (\alpha = 1, 2), \\ [a]_{21}^{(1)} + [b]_{21}^{(1)} = 0, \\ [c]_{11} = [c]_{12} = [c]_{21} = 0. \quad (\text{A9})$$

We now compute the integrals combining them in pairs:

$$[a]_{22}^{(1)} + [b]_{22}^{(1)} = \frac{(a-d)(a-2)c}{4dT\hat{m}^{2\delta}} R_2^{(4)}(0)^2 (\nabla u_x)^2 \times \int_{\{q\}} \left[\frac{1}{(q_1 + q_2)^2 + 1} - \frac{1}{q_2^2 + 1} \right] \frac{q_1^{a-d-2} q_2^{a-d}}{(q_1^2 + 1)^2}, \quad (\text{A10})$$

where we have included $1/c^2$ in redefinition of $R_i(u)$. The integral over q_i in Eq. (A10) is of order $O(1/\varepsilon)$ so that $[a]_{22}^{(1)} + [b]_{22}^{(1)}$ is finite and does not correct elasticity at two-loop order. Other diagrams give

$$[a]_{12}^{(2)} + [b]_{12}^{(2)} = \frac{c(\nabla u_x)^2 (a-d)(a-2)}{2T} \hat{m}^{-(\varepsilon+\delta)} \times (J_1 - J_2) R_1''(0) R_2^{(6)}(0), \quad (\text{A11})$$

$$[a]_{22}^{(2)} + [b]_{22}^{(2)} = \frac{c(\nabla u_x)^2 (a-d)(a-2)}{2T} \hat{m}^{-2\delta} \times (J_3 - J_4) R_2''(0) R_2^{(6)}(0), \quad (\text{A12})$$

where we have defined the following two-loop integrals:

$$J_1 = \int_q \frac{q_2^{a-d-2}}{(1+q_1^2)^2 [1+(q_1+q_2)^2]} = \frac{K_4^2}{\delta(\delta+\varepsilon)} + O(\varepsilon^{-1}, \delta^{-1}), \\ J_2 = \int_q \frac{q_2^{a-d-2}}{(1+q_1^2)^2 (1+q_2^2)} = \frac{K_4^2}{\delta\varepsilon} + O(\varepsilon^{-1}, \delta^{-1}), \\ J_3 = \int_q \frac{q_1^{a-d} q_2^{a-d-2}}{(1+q_1^2)^2 [1+(q_1+q_2)^2]} = \frac{K_4^2}{2\delta^2} + O(\varepsilon^{-1}, \delta^{-1}), \\ J_4 = \int_q \frac{q_1^{a-d} q_2^{a-d-2}}{(1+q_1^2)^2 (1+q_2^2)} = \frac{K_4^2}{\delta^2} + O(\varepsilon^{-1}, \delta^{-1}). \quad (\text{A13})$$

The last diagram

$$[c]_{22} = -\frac{(a-d)^2 c}{2dT\hat{m}^{2\delta}} R_2^{(4)}(0)^2 (\nabla u_x)^2 \times \int_{\{q\}} \frac{[q_1 \cdot q_2] q_1^{a-d-2} q_2^{a-d-2}}{[(q_1 + q_2)^2 + 1] (q_1^2 + 1) (q_2^2 + 1)} \quad (\text{A14})$$

is finite in the limit $\varepsilon, \delta \rightarrow 0$, and thus does not correct elasticity at two-loop order.

¹ S. Lemerle, J. Ferre, C. Chappert, V. Mathet, T. Giamarchi, and P. Le Doussal, Phys. Rev. Lett. **80**, 849 (1998).

² G. Grüner, Rev. Mod. Phys. **60**, 1129 (1988).

³ G. Blatter, M.V. Feigel'man, V.B. Geshkenbein, A.I. Larkin, and V.M. Vinokur, Rev. Mod. Phys. **66**, 1125 (1994).

⁴ D. S. Fisher, Phys. Rep. **301**, 113 (1998).

- ⁵ M. Kardar, Phys. Rep. **301**, 85 (1998).
- ⁶ S. Brazovskii and T. Nattermann, Adv. Phys. **53**, 177 (2004).
- ⁷ T. Giamarchi and P. Le Doussal, Phys. Rev. Lett. **72**, 1530 (1994); Phys. Rev. B **52**, 1242 (1995).
- ⁸ L. Civalle, A.D. Marwick, T.K. Worthington, M.A. Kirk, J.R. Thompson, L. Krusin-Elbaum, Y. Sun, J.R. Clem, and F. Holtzberg, Phys. Rev. Lett. **67**, 648 (1991).
- ⁹ D.R. Nelson and V.M. Vinokur, Phys. Rev. Lett. **68**, 2398 (1992).
- ¹⁰ L. Radzihovsky, Phys. Rev. Lett. **74**, 4923 (1995).
- ¹¹ A.W. Smith, H.M. Jaeger, T.F. Rosenbaum, W.K. Kwok, and G.W. Crabtree, Phys. Rev. B **63**, 064514 (2001).
- ¹² T. Hwa, D.R. Nelson, and V.M. Vinokur, Phys. Rev. B **48**, 1167 (1993).
- ¹³ R.J. Olsson, W.K. Kwok, L.M. Paulius, A.M. Petrean, D.J. Hofman, and G.W. Crabtree, Phys. Rev. B **65**, 104520 (2002).
- ¹⁴ G. Refael, W. Hofstetter, and D.R. Nelson, Phys. Rev. B, **74**, 174520 (2006).
- ¹⁵ M. Mezard and G. Parisi, J. Phys. A **23**, L1229 (1990).
- ¹⁶ D. S. Fisher, Phys. Rev. Lett. **56**, 1964 (1986).
- ¹⁷ A.I. Larkin, Sov. Phys. JETP **31**, 784 (1970).
- ¹⁸ T. Nattermann, S. Stepanow, L.-H. Tang, and H. Leschhorn, J. Phys. II **2**, 1483 (1992).
- ¹⁹ H. Leschhorn, T. Nattermann, S. Stepanow, and L.-H. Tang, Ann. Phys. **6**, 1 (1997).
- ²⁰ O. Narayan and D. S. Fisher, Phys. Rev. B **48**, 7030 (1993).
- ²¹ A.A. Fedorenko and S. Stepanow, Phys. Rev. E **67**, 057104 (2003).
- ²² P. Chauve, P. Le Doussal, and K.J. Wiese, Phys. Rev. Lett. **86**, 1785 (2001).
- ²³ P. Le Doussal, K.J. Wiese, and P. Chauve, Phys. Rev. B **66**, 174201 (2002).
- ²⁴ P. Le Doussal, K.J. Wiese, and P. Chauve, Phys. Rev. E **69**, 026112 (2004).
- ²⁵ P. Le Doussal, M. Mueller, and K.J. Wiese, Phys. Rev. B **77**, 064203 (2008).
- ²⁶ L. Roters and K.D. Usadel, Phys. Rev. E **65**, 027101 (2002)
- ²⁷ L. Roters, S. Lübeck, and K. D. Usadel, Phys. Rev. E **66**, 026127 (2002).
- ²⁸ A. Rosso, A.K. Hartmann, and W. Krauth, Phys. Rev. E **67**, 021602 (2003).
- ²⁹ A. Rosso, W. Krauth, P. Le Doussal, J. Vannimenus, and K.J. Wiese, Phys. Rev. E **68**, 036128 (2003).
- ³⁰ A.A. Fedorenko, P. Le Doussal, and K.J. Wiese, Phys. Rev. E **74**, 041110 (2006).
- ³¹ A.A. Middleton, P. Le Doussal, and K.J. Wiese, Phys. Rev. Lett. **98**, 155701 (2007); P. Le Doussal and K.J. Wiese, EPL **77**, 66001 (2007); A. Rosso, P. Le Doussal, and K.J. Wiese, Phys. Rev. B **75**, 220201(R) (2007).
- ³² L. Balents, Europhys. Lett. **24**, 489 (1993).
- ³³ P. Chauve, P. Le Doussal, and T. Giamarchi, Phys. Rev. B **61**, R11906(2000).
- ³⁴ P. Chauve, Ph.D. thesis, Université de Paris XI Orsay, 2000; <http://www.lpt.ens.fr/~chauve/>
- ³⁵ A.A. Fedorenko, P. Le Doussal, and K.J. Wiese, Phys. Rev. E **74**, 061109 (2006).
- ³⁶ S.N. Dorogovtsev, Phys. Lett. **76A**, 169 (1980).
- ³⁷ D. Boyanovsky and J.L. Cardy, Phys. Rev. B **26**, 154 (1982).
- ³⁸ A.A. Fedorenko, Phys. Rev. B **69**, 134301 (2004).
- ³⁹ A. Weinrib and B.I. Halperin, Phys. Rev. B **27**, 413 (1983).
- ⁴⁰ E. Korutcheva and F. Javier de la Rubia, Phys. Rev. B **58**, 5153 (1998).
- ⁴¹ V.V. Prudnikov and A.A. Fedorenko, J. Phys. A **32**, L399 (1999); V.V. Prudnikov, P.V. Prudnikov, and A.A. Fedorenko, *ibid.* **32**, 8587 (1999); Phys. Rev. B **62**, 8777 (2000).
- ⁴² A.A. Fedorenko and F. Kühnel, Phys. Rev. B, **75**, 174206 (2007).
- ⁴³ Y. Yamazaki, A. Holz, M. Ochiai, and Y. Fukuda, Physica A **150**, 576 (1988).
- ⁴⁴ Y. Nonomura and X. Hu, Europhys. Lett. **65**, 533 (2004).
- ⁴⁵ C. Dasgupta and O.T. Valls, Phys. Rev. B **72**, 094501 (2005).
- ⁴⁶ P. Chauve, T. Giamarchi, and P. Le Doussal, Phys. Rev. B **62**, 6241 (2000).
- ⁴⁷ J.L. Cardy and S. Ostlund, Phys. Rev. B **25**, 6899 (1982); P. Le Doussal and G. Schehr, *ibid.* **75**, 184401 (2007).
- ⁴⁸ I. Affleck, W. Hofstetter, D.R. Nelson, and U. Schollwöck, J. Stat. Mech.: Theory Exp. 2004, P10003.
- ⁴⁹ F.D.M. Haldane, Phys. Rev. Lett. **47**, 1840 (1981).
- ⁵⁰ J.P. Rodriguez and M.P. Maley, Phys. Rev. B **73**, 094502 (2006); J.P. Rodriguez, *ibid.* **76**, 224502 (2007).
- ⁵¹ M. Kardar, G. Parisi, and Y.-C. Zhang, Phys. Rev. Lett. **56**, 889 (1986).
- ⁵² E. Medina, T. Hwa, M. Kardar, and Y.-C. Zhang, Phys. Rev. A **39**, 3053 (1989).
- ⁵³ C.-H. Lam, L.M. Sander, and D.E. Wolf, Phys. Rev. A **46**, R6128 (1992).
- ⁵⁴ E. Katzav and M. Schwartz, Phys. Rev. E **70**, 011601 (2004).